(12)

FURTHER MODELING OF TURBULENT WALL PRESSURE ON A CYLINDER AND ITS SCALING WITH DIAMETER

David M. Chase

Tech Memo 21

Contract N00014-80-C-0730

C. I. Job 012

19 December 1981

Submitted to:

Dr. Peter H. Rogers
Code 421
Office of Naval Research
800 North Quincy Street
Arlington, VA 22217

Submitted by:

Chase Inc.
14 Pinckney Street
Boston, MA 02114

Errata for "Further modeling of turbulent wall pressure on a cylinder and its scaling with diameter" by D. M. Chase, Chase Inc. TM 21, December 1981

p. 18, line (-3): For "Ref. 20" read "Ref. 3".

p. 19, Eq. 32a: Replace expression for C' by

$$C' = \ell n\,|(k^2-\omega^2/c^2)^{\frac{1}{2}}a| - 0.116-i\alpha.$$

This correction results from a corresponding correction in Eq. 62 and certain earlier equations in Ref. 3.

ABSTRACT

The possible scaling of the axisymmetric component of spectral density of wall pressure in turbulent flow along a slender cylinder is reexamined with use of a formal low-wavenumber expansion in terms of fluctuating Reynolds stresses as sources. A rudimentary model of the sources is formed that conforms to the principle of local similarity near the wall and to probable implications of fluctuating and mean velocity profiles measured in cylindrical boundary layers. To the extent that wall pressure is exclusively due to such a turbulence field, to zero order in wavenumber, at least, it is indicated to scale with cylinder radius (a) and to agree in functional dependence with the current model for this low-wavenumber component. If the turbulence field (despite lack of experimental evidence) involves in addition a weak component that scales with boundary-layer thickness, then at sufficiently low frequencies and wavenumbers the corresponding contribution to wall pressure (when $\delta/a>>1$) may become dominant, and the extrapolation of the current model to very small $\omega a/U_\infty$ and the associated prediction of diameter dependence may then fail.

TABLE OF CONTENTS

1. INTRODUCTION

The question of accurate and validated modeling of the axisymmetric component of turbulent wall pressure on a towed flexible cylinder remains one of intense interest. Apart from elements of uncertainty in the parameter domain of common concern, it is becoming important to extrapolate into diameter/speed/frequency domains where the experimental basis for modeling is more indirect and less secure. Such modeling is needed to predict prospective performance in future innovative as well as more conventional improved systems and thus to guide development.

In this regard the question particularly arises as to whether a current tentative model for the wavenumber-frequency spectral density of the subject axisymmetric harmonic of wall pressure, $P_0(k,\omega)$, incorporating as the sole pertinent length scale the cylinder radius, a, is likely to provide a correctly indicative result when extrapolated to very small values of $\omega a/U_\infty$. This memo attempts further discussion of this topic by reference especially to available measurements and further plausible modeling of turbulent flow at large values of δ/a, the ratio of boundary-layer thickness to cylinder radius. This represents a line of development based in part also on previous formal and semiempirical modeling pursued in the ONR program (see especially Refs. 1-3).

A more complete application of current modeling to measured noise in high-speed towing tests of quiet modules than that undertaken in Ref. 2 is also needed. In particular, the preliminary analysis of data from the LSM used a simplified and somewhat inadequate representation of the wavenumber filtering action of the specially mounted hydrophone employed. Such further application of modeling may be undertaken in towed-array exploratory development outside the scope of the more basic ONR program and would be complementary to the present work. An updated appraisal of the residual noise level attainable by towed arrays could then also be performed.

A related question not addressed further here is whether, for given speed and streamwise position along a cylinder, there is a diameter below which the flow is no longer fully turbulent. Suggested criteria for such a diameter (or related Reynolds number) have been reviewed in Ref. 30 (p. 124), but later measurements discussed in Ref. 19 (pp. 22-23) indicate that a transition diameter, if it exists at all, may be exceedingly small.* Below such a transition threshold, the present semi-empirical modeling and resulting scaling of wall pressure for turbulent flow would not apply.

2. ELEMENTS OF PREVIOUS MODELING AND THE POSSIBLE ROLE OF DISTINCT LENGTH SCALES

Initially, attention is restricted to the form of $P_0(k,\omega)$ at negligible wavenumber, i.e. $P_0(0,\omega)$. According to the current model

$$P_0(0,\omega) = C\rho^2 v_*^3 a^{-3} (\omega/v_* + h/ba)^{-5}, \qquad (1)$$

where C and h/b are numerical constants and v_* is identified as the wall friction velocity and taken proportional to U_∞, say

*For a cylinder in water at a flow speed of 15 kt, for example, it is indicated that the transition diameter is $\lesssim$ 0.01 cm.

$v_* = 0.04U_\infty$. Though this form was suggested by rudimentary modeling considerations, it is supported mainly by inference from certain noise measurements within liquid-filled towed-array modules. Indications have been adduced that the appropriate length scale in $P_0(k,\omega)$ is cylinder radius, as implied by Eq. 1, and the preliminary analysis of measurements in the LSM,[23] a module of larger radius, indicated rough consistency with the notion of a as the length scale and with the model form of $P_0(k,\omega)$ that underlies Eq. 1 (see Sec. 3). Nevertheless, these indications are not yet uniquely compelling, and the form (1) presently rests mainly on a single module, XN-55.[24]

Model (1) or any model of $P_0(0,\omega)$ based on a single length (and velocity) scale has the form[4]

$$P_0(0,\omega) = \rho^2 v_*^3 a^2 F(\omega a/v_*) \ . \qquad (2)$$

From an uninformed point of view, it may naturally be asked whether in a more exact model there may not be included additively in $P_0(0,\omega)$ a similar second term, $\rho^2 v_*^3 \delta^2 G(\omega\delta/v_*)$, say, that scales rather on boundary-layer thickness. Suppose, as a conjectural example, that these two functions F and G each had the dependence implied in Eq. 1, so that one might write

$$P_0(0,\omega) = \rho^2 v_*^3 [C_1 a^{-3}(\omega/v_* + h_1/b_1 a)^{-5} + C_2 \delta^{-3}(\omega/v_* + h_2/b_2\delta)^{-5}]. \qquad (3)$$

If the respective intensity and scale coefficients satisfy the conditions

$$C_1 >> (a/\delta)^8 C_2 \quad \text{but} \quad C_1 (b_1/h_1)^5 << (\delta/a)^2 C_2 (b_2/h_2)^5$$

(as would be so if, for example, $\delta >> a$ and $C_1 \sim C_2$, $b_1 \sim b_2$, $h_1 \sim h_2$), then the δ-scaled contribution would become dominant at sufficiently

small $\omega a/v_*$ even though the a-scaled contribution was dominant at greater values, including even a plateau interval, as shown in the sketch below. In such event, extrapolation to lower

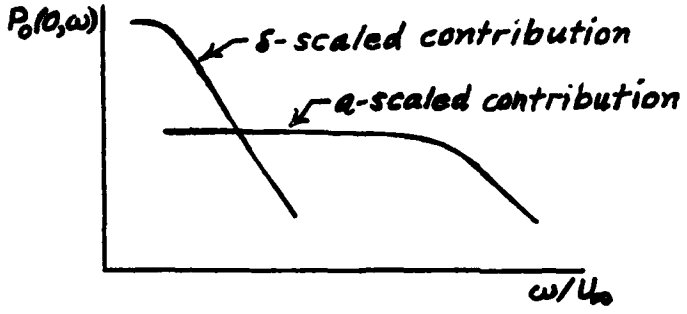

diameter-frequency products on the basis of a model fit to measurements in the range of dominance by the a-scaled contribution could grossly underestimate the noise below the steep rise due to the δ-scaled contribution. In particular, the dependence of $P_0(0,\omega)$ on a as a^2 for $b_1\omega a/h_1 v_* \lesssim 1$ predicted from the a-scaled contribution alone would be replaced by independence of a at values of a small enough that the δ-scaled part became dominant.

The preceding hypothetical account, though illustrative, is oversimplified and, if valid at all, requires modification. In particular, even a contribution to axisymmetric wall pressure associated with a fluctuating velocity that scales with δ may involve also cylinder radius, on account of its geometric role, contrary to the form of the second term in (3). Hence, in addition to delineating and modeling possible scaling properties of the turbulent boundary layer in the light of present understanding of wall turbulence and measurements in cylindrical geometry, it is required to invoke an explicit formal relation of axisymmetric wall pressure to the turbulent velocity field. This is pursued in Sec. 4.

If a model spectrum with additive terms characterized respectively by turbulence scales a and δ (with additional geometric dependence of both terms on a) is a viable possibility, there is no suggestion of it, at least, in the profile of the rms streamwise component u of fluctuating velocity in the boundary layer on a thin cylinder measured by Leehey and Stellinger.[5] (See Fig. 1, repeating Ref. 6, Fig. 2.3-6, based on Ref. 5, Fig. 8.) This profile, apart from the rise in the viscous sublayer and a peak somewhat outside it, conforms well, as shown and analyzed by Kronauer,[6] to dependence as $r^{-\frac{1}{2}}$, i.e. $u \propto v_* (a/r)^{\frac{1}{2}}$, all the way to $r \approx 26a$, while in the subject case the edge of the boundary layer falls at $r \approx 44a$. Clearly (though even prior to seeing the measured profile it would perhaps be naive to imagine the turbulent dynamics to permit it) there is not a contribution to the profile ($\propto r^{-\frac{1}{2}}$) that extends only to a distance that is a modest multiple of a and is associated with turbulent motion with scale ~a, followed at larger wall distances by a distinct contribution that extends to $r \sim \delta$ and is associated with a turbulent motion of scale ~δ.

On the other hand, despite the cited monolithic profile, a contention might be made, along the lines of the discussion by Bradshaw,[7] following Townsend,[8] referring in their case to planar turbulent boundary layers with or without mean pressure gradient, that the turbulence is nevertheless composed of two such components of disparate scales. The large-scale wake-like component, described as "inactive," would be thought not to transfer much momentum nor to interact appreciably with the "universal" component, which would scale rather with distance y from the wall when $y \lesssim a$. Part of the modeling introduced below is intended to reflect this possible contention.

3. SELECTIVE REVIEW OF MODELING PRESSURE ON A CYLINDICAL WALL

Elements of previous modeling will now be further outlined. In Ref. 9 (but based on the earlier Ref. 10) a type of model was advanced for the azimuthal harmonic spectral densities $P_m(k,\omega)$ (m integer) of turbulent wall pressure on a cylinder by writing

$$P_m(k,\omega) = \int_{(m-\frac{1}{2})/a}^{(m+\frac{1}{2})/a} dk_3 P(k,k_3,\omega) \qquad (4)$$

and choosing a model spectral density $P(k,k_3,\omega)$, which depends on a second wavenumber analogous to the transverse component in the instance of a planar boundary. For the planar case a theoretically attractive model for the wavevector-frequency spectral density of wall pressure in the low-wavenumber domain that conformed as well as any to the laboratory measurement of low-wavenumber planar wall pressure by Jameson[12] was the scale-independent, wavenumber-quadratic one of the form

$$P(k_1,k_3,\omega) = C_2 \rho^2 v_*^5 \omega^{-3} (v_* K/\omega)^2, \quad K^2 \equiv k_1^2+k_3^2 \qquad (5)$$

(C_2 constant). Eqs. 4 and 5 yielded for application in some domain restricted at least by the condition $k \lesssim \omega/U_\infty$,

$$P_0(k,\omega) = C_2 \rho^2 v_*^8 \omega^{-5} a^{-1} (k^2+\frac{1}{12} a^{-2}) . \qquad (6)$$

A trial model to encompass the full wavenumber/frequency domain of interest, including the convective one, was constructed, in effect, as follows. The spectral density of wall pressure for a frame convecting downstream at some speed u_c is obtained from (6) by replacing ω by $\omega-u_c k$. Suppose that in that frame, for suitably chosen u_c, the decorrelation of axisymmetric wall

pressure due to streamwise separation ζ is comparable with that due instead to time delay τ if ζ and τ are related by a dispersion velocity scale $\sim v_*$, i.e. if $\zeta \sim v_* \tau$, and suppose that, for separation and time delay both nonvanishing, the decorrelating effects add in quadrature (see also Refs. 11, 21). If the decorrelation is also scale-independent, we have then to replace ω/v_* in Eq. 6 by

$$k_+ \equiv [(\omega - u_c k)^2/(hv_*)^2 + k^2]^{\frac{1}{2}} , \tag{7}$$

where h is of the order of unity. For sufficiently low frequencies $|\omega - u_c k|$ and wavenumbers k, however, a cutoff of the rise in the pressure spectrum must be effected by the finite scale, say Δ, of the largest contributing turbulent motions. Originally, it was assumed for convenience that this cutoff wavenumber, Δ^{-1}, could be added in quadrature with the frequency-augmented wavenumber (7), so that the generalized model based on Eq. 6 became

$$P_0(k,\omega) = C_2 \rho^2 v_*^3 a^{-1} (k^2 + \frac{1}{12} a^{-2}) [(\omega - u_c k)^2/(hv_*)^2 + k^2 + \Delta^{-2}]^{-5/2} \tag{8}$$

When this model was applied to infer turbulence-induced noise within a liquid-filled hose and results compared to various test measurements most suitable among those then available, the indicated magnitude of the level coefficient C_2 in (8) proved—possibly fortuitously but certainly encouragingly—to have approximately the value inferred for C_2 in the underlying planar model (5) on the basis of Jameson's measurements. When measurements became available in quieter small-diameter liquid-filled modules, notably XN-55, especially at higher speeds, however, it was found that the inferred form of $P_0(0,\omega)$ would be appreciably better matched if the model (8) was altered simply by assuming the wavenumber scale Δ^{-1} to enter the wavenumber denominator linearly instead of in quadrature, yielding

$$P_0(k,\omega) = C_2 \rho^2 v_*^3 a^{-1} (k^2 + \tfrac{1}{12} a^{-2}) \{ [(\omega - u_c k)^2/(hv_*)^2 + k^2]^{\frac{1}{2}} + \Delta^{-1} \}^{-5} . \quad (9)$$

This form, though mathematically less convenient than (8), seems more likely also on the basis of possible explicit source modeling.

The relation (4), if $P(k,k_3,\omega)$ is identified with the true spectral density $P(k_1,k_3,\omega)$ for a planar boundary, clearly ensures consistency of the $P_m(k,\omega)$ with the result required in the planar limit defined by $\delta/a \to 0$, $ka \to \infty$, $\omega a/v_* \to \infty$, in which the discrete circumferential wavenumber components m/a become closely spaced compared with all pertinent wavenumbers. The minimum necessary limiting condition of correspondence between the $P_m(k,\omega)$ and $P(k_1,k_3,\omega)$ does not seem obvious, however, and may be much weaker than that implied by Eq. 4. For example, as noted more explicitly in Ref. 2 (footnote, pp. 15-16) there may be no unique correspondence referring to a single, finite value of m. The original postulated relation (4) thus may not be valid even as a limiting approximation, at least when m = 0. Correspondingly, the modeling analysis of Ref. 1 (even without the specialized modeling assumptions therein) indicated no basis for the specific form $a^{-2}[1/12+(ka)^2]$ of the parenthetical factor that entered Eqs. 6, 8, and 9. It suggested that in trial modeling the quantity $1/12+(ka)^2$ be replaced by a somewhat more general polynomial in ka.

For reference, the trial model form we presently employ is given by

$$P_0(k,\omega) = C_2 \rho^2 v_*^3 a^{-1} (a^{-2} + s_2 k^2) \{ [(\omega - u_c k)^2/(hv_*)^2 + k^2]^{\frac{1}{2}} + \Delta^{-1} \}^{-5} \quad (9a)$$

with $\Delta = ba$.*

*Apart from any more general modification that may prove necessary, presence of a term linear in k in addition to $a^{-2} + s_2 k^2$ is not excluded.

Regarding the length scale Δ entering $P_0(k,\omega)$, apart from the as yet imperfect analysis of the implications of parallel comparisons with noise measured in modules of different diameters, alluded to above, other indications and suggestions were drawn. Measurements of frequency spectra of wall pressure by small (not axisymmetric) flush hydrophones at various positions along a towed cylinder were made by Markowitz.[14] As noted in Ref. 14 (see also Ref. 9), these conformed more nearly to scaling with radius a than with layer thickness δ,* and measurements by other workers were consistent with such a result when $\delta/a>>1$. It was proposed in Ref. 16 (see also Ref. 9) that a model wall pressure with a single scale Δ, e.g. as in Eq. 9, would suffice, but this scale would depend on both a and δ, becoming $\propto\delta$ in the limit where $\delta/a\to 0$ and increasing more strongly with a than with δ where $\delta/a>>1$.

4. FORMULATION OF MODEL SOURCE SPECTRA FOR APPLICATION TO WALL PRESSURE

Recent work in the present program provides the formal relation of the subject pressure spectrum $P_0(k,\omega)$ to source spectra solely of fluctuating velocity products (Reynolds stresses).[3] This seems likely to be a safer approach (i.e., less likely to mislead) than that based on the Poisson equation for pressure (in incompressible flow). The latter involves also, apart from spectra of two-component velocity products, in connection with a mean-flow interaction term, a spectrum of (single-component) fluctuating velocity normal

*The measured frequency-spectral dependences were not closely consistent, however, with the present model or with general theoretical expectations for turbulent wall pressure.

to the wall. This approach was formulated in cylindrical geometry in Ref. 1 and pursued for a specific source model.

The present approach via pure velocity-product sources permits straightforward approximation of the pertinent Green's function required to exhibit wall pressure explicitly in terms of assumed sources only in the nonconvective tail ($U_\infty|k| \lesssim \omega$). An explicit result has been given only where, in addition, $|k|\delta \lesssim 1$. Resulting modeling may guide expectations, however, also outside this domain. At the present time, it should be mentioned, formal results of the respective approaches in this domain exhibit apparent differences that remain to be elucidated.

The relations from Ref. 3 to be used are available in a form sufficiently general to include slightly compressible flow. This generalization is worth having though beside the point of the present considerations.

At k=0, i.e. to lowest order in k, axisymmetric wall-pressure amplitude is related to amplitudes $\hat{T}_{rr}^{0}(r,k,\omega)$, $\hat{T}_{\theta\theta}^{0}(r,k,\omega)$ (with k=0) of the self products of radial and of azimuthal fluctuating velocity at radius r (wall distance r-a), according to Ref. 3, Eq. 62 (or Ref. 1), by

$$\hat{p}_0(0,\omega) = \rho\int_a^\infty drr^{-1}(\hat{T}_{rr}^{0}-\hat{T}_{\theta\theta}^{0}) \ . \qquad (10)$$

If we imagine the higher-order terms in k also to be included, it is sensible to retain the argument k of the $\hat{T}_{ii}$ rather than setting k=0. In fact, since we can only try to find support or motivate modification of current model forms—not pursue rigorous expansions—and we wish to do this with regard to their full domain of hypothetical applicability, we feel free to model the spectra of $\hat{T}_{ii}$ as though encompassing also the convective domain.

The spectral density at k = 0 is given by Eq. 10 as

$$P_0(0,\omega) = \rho^2\int_a^\infty drr^{-1}\int_a^\infty drr'r'^{-1}E_0(r,r',0,\omega) \ , \qquad (11)$$

where $E_0(r,r',k,\omega)$ denotes the (cross) spectral density associated with $\hat{T}^0_{rr}-\hat{T}^0_{\theta\theta}$. (Index zero here refers to m.) In accord with the preceding discussion, we wish to consider the right member of (11) also for general k and denote the result by

$$P^0_0(k,\omega) = \rho^2\int_a^\infty drr^{-1}\int_a^\infty dr'r'^{-1}E_0(r,r',k,\omega). \tag{12}$$

First, however, we consider the formation of a plausible type of model for spectra $E^m_{11}(r,r',k,\omega)$ of the streamwise fluctuating velocity component. The corresponding profile of the single-point rms value,

$$E_{11}(r) = \sum_{m=-\infty}^{\infty} E^m_{11}(r), \quad \text{where } E^m_{11}(r) = \int d\omega\int dk E^m_{11}(r,r,k,\omega), \tag{13}$$

has been measured,[5] as noted in Sec. 2. This is intended to guide analogous modeling of velocity-product spectra, notably $E_0(r,r',k,\omega)$ that appears in Eq. 12. The model is required to claim validity even where $r,r' \gtrsim a$ when $\delta/a>>1$.

We consider a model characterized by a single length scale, Δ, but spectra may also be formed by "incoherent" addition of such spectra having different scales (cf. Sec. 2). In the spirit of our usual modeling assumptions we suppose that E^0_{11} (and likewise velocity-product spectra such as E_0) depends on ω and k only via k_+, defined by Eq. 7. We may then write

$$E^0_{11}(r,r',k,\omega) = v_*\Delta^2(a/r)^{\frac{1}{2}}(a/r')^{\frac{1}{2}}F^0_{11}(k_+(rr')^{\frac{1}{2}},k_+(r'-r),k_+\Delta). \tag{14}$$

The profile factor $(a^2/rr')^{\frac{1}{2}}$ is required to conform to the measured dependence of $E_{11}(r)$ as a/r (for $r\lesssim\delta$ except near the wall, Fig. 1), at least for the class of functions F^0_{11} (and their generalization, F^m_{11}, to $m\neq 0$) considered here.

A suggestive approach to a type of model for F^m_{11} (especially when $\delta >> a$) may be based on imagining first a region of more or less homogeneous turbulence of fixed scale Δ without regard to presence of a physical cylinder. The fluctuating velocity field may then be imagined expanded in waves of definite k and ω and angular harmonics m defined for a cylindrical coordinate system. If a model is assumed for wavevector-frequency spectra of fluctuating components appropriate to the hypothetical turbulent field, this may thus be expressed by explicit transformation in terms of spectral components characterized by m,k,ω,r,r'.

To treat the actual case where a hard cylinder is present and responsible for generating the turbulent field by its motion, the essential step is to permit the scale Δ in the formally constructed model to depend on the distances $y \equiv r-a$, $y' \equiv a'-a$ from the wall. For $y=y'<<a$ (but outside the sublayer), in particular, the usual similarity principle for a planar wall [7,17] implies that $\Delta \propto y$. (We look apart, for the moment, from any weak inactive component scaling otherwise.)

Proceeding along these lines, as shown somewhat more explicitly in Appendix 1, an indicative class of models may be characterized (leaving aside the choice of Δ) by regarding the function F^0_{11} in Eq. 14 as given roughly in opposite limiting domains by

$$S_1(k_\Delta \Delta_r) \times \begin{cases} 1 , & k_\Delta (rr')^{\frac{1}{2}} \lesssim 1 \\ B[k_\Delta (rr')^{\frac{1}{2}}]^{-1} , & k_\Delta (rr')^{\frac{1}{2}} \gtrsim 1 , \end{cases} \tag{15}$$

where

$$k_\Delta \equiv (k_+^2 + b_0^2 \Delta^{-2})^{\frac{1}{2}} , \quad \Delta_r \equiv [(r'-r)^2 + b_1^2 \Delta^2]^{\frac{1}{2}} , \tag{15a}$$

and b_0, b_1 are constants.* The function $S_1(z)$ in (15) approaches a constant (of the order of unity) for arguments $z \lesssim 1$ and decreases at some rapid rate for $z \gtrsim 1$.

*Either b_0 or b_1 could be absorbed in the definition of Δ, but it is convenient for consideration of models where $b_0 \to 0$ or $b_1 \to 0$ to preserve their explicit appearance.

On the basis of properties of a function found in Ref. 11 to fit measurements by Bullock, Cooper, and Abernathy[18] of cross-spectra ($y'-y\neq 0$) of streamwise turbulent velocity over an effectively planar wall, we assume that $b_0 = 0$ in (15a). (A certain illustrative model with $b_0\neq 0$ but $b_1=0$ is also considered to some extent in Appendix 1.) The requisite estimates based on the model are greatly facilitated thereby.

We turn to modeling of velocity-product spectra such as E_0 in Eq. 12. In view of the quadratic dependence of these products on individual velocity components and the expectation that their spectra resemble that of streamwise velocity in their dependence in limiting domains of the arguments (e.g. for $k_\Delta \Delta_r \lesssim 1$ or $\gtrsim 1$), we assume that model equations exactly analogous to (14) and (15) for E^0_{11} apply to E_0 where the square of the previous profile factor must be used:

$$E_0(r,r',k,\omega) = v_*^3\Delta^2(a/r)(a/r')F_0(k_+(rr')^{\frac{1}{2}},\ k_+(r'-r),\ k_+\Delta)\ , \qquad (16)$$

where F_0 is characterized again as in (15) with S_1 replaced by, say, S_0.

For present indicative estimation of limiting dependences we interpolate in r,r' between opposite limiting domains of $k_\Delta(rr')^{\frac{1}{2}}$ in (15) by assuming a convenient product form

$$F_0 = (1+\alpha k_\Delta r)^{-\frac{1}{2}}(1+\alpha k_\Delta r')^{-\frac{1}{2}}S_0(k_\Delta \Delta_r) \qquad (17)$$

($\alpha^2 = B^{-1}$).* More significantly, we wish to assume also a factorable form for S_0. In this connection, we note, in S_1 referring to the

*Possible different presumptions include that $F=[1+\alpha k_\Delta (rr')^{\frac{1}{2}}]^{-1} S_0$.

spectrum of (linear) streamwise velocity, the earlier fit[11] to the measurements of Ref. 18 corresponded to taking $\Delta = (yy')^{\frac{1}{2}}$, $b_1 = \sqrt{2}$ (and $k_\Delta = k_+$) (in 15a), so that $\Delta_r = (y^2+y'^2)^{\frac{1}{2}}$. If the same assumption is appropriate for S_0, referring to a spectrum of velocity products, and if one had $S_0(k_+\Delta_r) \propto \exp[-(\beta k_+\Delta_r)^2]$ (β=const.), for example, then $S_0 \propto \exp[-(\beta k_+ y)^2]\exp[-(\beta k_+ y')^2]$, a product form. Actually, the fitted S_1 did not have such a Gaussian form. Still, it is perhaps indicative of limiting dependences to assume a product form:

$$S_0(k_+\Delta_r) = S(k_+y)S(k_+y') \ , \tag{18}$$

where the function S(z) begins to decrease rapidly for z greater than a value of the order of unity. It is tentatively assumed also that, for all k and ω, the source spectrum is negligible outside the boundary-layer thickness, so that (notwithstanding its single indicated argument) the function $S(k_+y) = 0$ for $y>\delta$. Finally, a factorable form is assumed also for Δ^2:

$$\Delta^2 = L(y)L(y') \ , \tag{19}$$

where L has dimensions of length.

Eqs. 12, 16, 17, and 18 yield for the "generalized" zero-order contribution $P_0^0(k,\omega)$ to the wall-pressure spectrum

$$P_0^0(k,\omega) = \rho^2 v_*^3 a^2 I^2(k,\omega) \ , \tag{20}$$

$$I(k,\omega) = \int_0^\delta dy[1+\alpha k_+(a+y)]^{-\frac{1}{2}}(a+y)^{-2}L(y)S(k_+y) \ . \tag{20a}$$

5. SPECIFICATION OF SCALING OF SOURCE SPECTRA AND RESULTS FOR MODEL WALL-PRESSURE SPECTRA

In the context of this memo a central question is how to model the scale Δ (or, under assumption (19), L). Apart from suggesting a favored rough dependence for Δ, we wish to explore the consequences of alternative assumptions. If attention were confined to $y,y' \lesssim a$, as noted above, for consistency with the principle of local similarity we should take for $\Delta(y,y')$ a homogeneous symmetric function of first degree in y,y', so that $\Delta(y,y) \propto y$. In modeling for a planar wall in Ref. 11 it was proposed that $\Delta \propto (yy')^{\frac{1}{2}}$. For $y,y' \gtrsim a$, looking apart from any possible "non-similar" component scaling on δ, the notion of a scale $\propto y$ (when $y' \propto y$) loses any claim to sensibility,[7] and the reduced influence of the wall as its distance y becomes large compared with the wall radius appears to imply that Δ should be taken a homogeneous function of first degree in a,y,y' that increases with y (for $y' \propto y$) more slowly than y.

We pursue as a representative model along this line one where L(y) is proportional to a "mixing length." This is conventionally defined such that its product by the local shear velocity at y yields the "eddy viscosity", ε; this in turn is conventionally defined such that its product by the local mean velocity derivative U'(y) in the cylindrical flow (and by density) yields the local shear stress. I.e.,

$$\varepsilon = L(\tau/\rho)^{\frac{1}{2}}, \tag{21a}$$

$$\tau = \rho \varepsilon U'. \tag{21b}$$

In the approximation of circumferential integrated shear force independent of wall distance, which, as discussed in Ref. 6, is supported by the measured fluctuating velocity profile measured in Ref. 5, one has

$$\tau = \rho v_*^2/(1+y/a). \tag{22}$$

Combining Eqs. 17 and 18 yields

$$L = (1+y/a)^{-\frac{1}{2}} v_*/U'(y). \qquad (23)$$

The profile U(y) for cylindrical flow outside the near-wall region (in the analog of the log region for planar wall) has been measured extensively (in certain domains of Reynolds number) by Willmarth *et al.*[19] and Leehey and Stellinger.[5] An indicative approximation to the measured U(y) is provided by "Rao's hypothesis" (see present Appendix 2); in the log layer this implies

$$U'(y) \simeq \frac{Av_*}{r\ell nr} = \frac{Av_*/a}{(1+y/a)\ell n(1+y/a)} \quad (A\simeq 2.5) . \qquad (24)$$

In this approximation Eq. 23 becomes

$$L = 0.4a\ell n(1+y/a)(1+y/a)^{\frac{1}{2}} \qquad (25)$$

or, in opposite limits,

$$L \to \begin{cases} 0.4y, & y/a<<1 \\ 0.4(ay)^{\frac{1}{2}}\ell n(1+y/a), & y/a>>1. \end{cases}$$

The latter form indicates that, apart from the weakly varying log factor, the local scale varies as the geometric mean of wall distance and cylinder radius. An empirical correction factor suggested for the Rao profile in Appendix 2 would introduce in the scale (25) a factor varying slightly with δ/a but approximately independent of y except near the wall. The square of this factor would then be adjoined to Eqs. 27, 36, and 39 below.

Insertion of the mixing length L of (25) into (20a) and use of the properties of S(z) (see Eq. 18) yields in opposite limiting domains, where for the case of interest it is assumed also that $a/\delta<<1$:

$$I \sim \begin{cases} \text{const.}\ , & k_+a<<1 \\ (k_+a)^{-5/2}\ , & k_+a>>1\ . \end{cases} \tag{26}$$

The result of (20) then accords with the limiting forms given by the term corresponding to $P_0^0(k,\omega)$ in the current a-scaled model (9a) (i.e. term a^{-2}, only, in the factor $a^{-2}+s_2k^2$). Otherwise stated, assumption of a particular interpolation form $I\sim(b^{-1}+k_+a)^{-5/2}$ consistent with the limiting forms (26) yields by (20)

$$P_0^0(k,\omega) = C_2\rho^2v_*^3a^{-3}[k_++(ba)^{-1}]^{-5}. \tag{27}$$

It is well to note results for $P_0^0(k,\omega)$ under alternative scaling assumptions. If in place of (25) L were taken to vary as y for $y\lesssim a$ but to become $\propto a$ for $y\gtrsim a$, the limiting forms (26) and hence a-scaling as in the current model would again apply. If L were taken (quite unjustifiably) to vary as y for all $y\lesssim\delta$, the constant I of (26) for $k_+a<<1$ would become instead $\sim\ell n(1+\delta/a)$ in the subrange $k_+\delta<<1$ and $\sim\ell n(1+1/k_+a)$ for $k_+\delta>>1$, with corresponding modifications implied in (27).

Suppose, on the other hand, that there is an inactive contribution to fluctuating velocity, as mentioned earlier, that scales entirely with δ and that no profile factor $(a/r)(a/r')$ applies to this component of E_0. Then $\Delta\propto\delta$ and, in place of (18), $S_0 = S_0(k_+\delta)$. Then in place of (20) and (20a) we obtain

$$P_0^0(k,\omega) = \rho^2v_*^3\delta^2I_\delta^2(k,\omega)S_0(k_+\delta) \tag{28}$$

$$I_\delta(k,\omega) = \int_0^\delta dy[1+\alpha k_+(a+y)]^{-\frac{1}{2}}(a+y)^{-1}. \tag{28a}$$

In limiting domains

$$I_\delta \sim \begin{cases} \ell n(1+\delta/a), & k_+a<<1,\ k_+\delta<<1 \\ \ell n(1+1/\alpha k_+a), & k_+a<<1<<k_+\delta \\ (k_+a)^{-\frac{1}{2}}, & k_+a>>1,\ k_+\delta>>1 \end{cases} \tag{29}$$

An example interpolation form then yields from (28)

$$P_0^0(k,\omega) = \rho^2 v_*^3 \delta^2 S_0(k_+\delta)\{k_+ + 1/a\ell n^2[1+(c_+k_+ + c_\delta \delta^{-1})^{-1} a^{-1}]\}^{-1}, \tag{30}$$

where c_+ and c_δ are constants. Setting $k_+ \to \omega/hv_*$ for $k=0$ yields the corrected form, under present assumptions, of the hypothetical second term in Eq. 3 for $P_0(0,\omega)$. In the extreme low-k, low-ω limit where $k_+\delta \lesssim 1$, in particular, the resulting equation then takes the form

$$P_0(0,\omega) = \rho^2 v_*^3 [C_1' a^2 + C_2' \delta^2 \ell n^2 (1+\delta/a)], \tag{31}$$

where C_1', C_2' are constants.

Such a hypothetical δ-scaled component of the turbulence might have somewhat the structure of the wake of an axisymmetric body, as suggested in Ref. 16. A model for the corresponding turbulent sources of pressure might be constructed somewhat as though this turbulence were homogeneous (modifying the similar course taken in Ref. 16 for wall pressure itself); this model form would differ somewhat from that taken in Eq. 28. In the absence of motivation by specific experimental results, detailed development of this kind seems unrewarding.

Reverting to the generalized similarity model that led to Eq. 27, we wish to consider also terms of higher order in k in the low-k expansion of $P_0(k,\omega)$. Eq. 62 of Ref. 20 for the two-term expansion of the amplitude $\hat{p}_0(k,\omega)$, from which the spectrum P_0 may be formed, may be written

$$\hat{p}_0(k,\omega) \to p_0^0(k,\omega) - 2\rho k \int_a^\infty dr\{\hat{T}^0_{\theta\theta}\omega^{-1}U'(r)[\ell n(r/a)+C'] - i\hat{T}^0_{rx}\}, \qquad (32)$$

where

$$C' = \ell n(\omega a/U_\infty) + \ell n|\omega/kU_\infty| + \tfrac{1}{2}\ell n|1-(\omega/ck)^2|^{-1} + 0.116 + i\alpha, \qquad (32a)$$

$$\hat{p}_0^0(k,\omega) = \rho\int_a^\infty dr r^{-1}(\hat{T}^0_{rr} - \hat{T}^0_{\theta\theta}) \ , \qquad (32b)$$

$\alpha = \pi/2$ or 0 for $|k| < \omega/c$ or $> \omega/c$, respectively, and it is understood that $\hat{T}^0_{ij} = \hat{T}'_{ij}(r,k,\omega)$ [cf. Eq. 10, in which $\hat{T}^0_{ij} = \hat{T}^0_{ij}(r,0,\omega)$]. $P^0(k,\omega)$, we recall, represents the spectral density formed from (32b) (see Eq. 12).

The term in (32) containing in its integrand a factor $\hat{T}^0_{rx}$ has the same form as the term (32b) already considered except that $\hat{T}^0_{rr} - \hat{T}^0_{\theta\theta}$ is replaced by $i2kr\hat{T}^0_{rx}$. The corresponding contribution to $P_0(k,\omega)$, say $P_0^{rx}(k,\omega)$ (excluding the cross-term between the $\hat{T}^0_{rx}$ term and other terms in Eq. 32), under assumptions similar to those leading to Eqs. 20, 20a, may similarly be written in the form

$$P_0^{rx}(k,\omega) = \rho^2 v_*^3 a^2 I^2_{rx}(k,\omega), \qquad (34)$$

$$I_{rx}(k,\omega) = k\int_0^\delta dy[1+\alpha k_+(a+y)]^{-\frac{1}{2}}(a+y)^{-1}L(y)S_{rx}(k_+y) \ , \qquad (34a)$$

where the dimensionless model source function S_{rx} is related to $i2\hat{T}^0_{rx}$ as $S(k_+y)$ was to $\hat{T}^0_{rr} - \hat{T}^0_{\theta\theta}$.

Assumption of the mixing length L of (25) as L(y) in (34a) and of properties of $S_{rx}(z)$ similar to those assumed above for S(z) yields in opposite limiting domains, where also $a/\delta \ll 1$,

$$I_{rx} \sim ka \times \begin{cases} (\delta/a)^{\frac{1}{2}} , & k_+\delta \ll 1 \\ (k_+a)^{-\frac{1}{2}} , & k_+a \ll 1 \ll k_+\delta \\ (k_+a)^{-5/2}, & k_+a \gg 1 \ . \end{cases} \qquad (35)$$

The corresponding limiting forms for P_0^{rx} given by (34) may be subsumed by an assumed interpolation to obtain

$$P_0^{rx}(k,\omega) \sim C\rho^2 v_*^3 a^{-3}(ka)^2[k_+ + (ba)^{-1}]^{-4}[k_+ + (b_\delta \delta)^{-1}]^{-1}, \quad (36)$$

where b_δ is a constant.

Finally, we consider the term in (32) explicitly proportional to $\hat{T}_{\theta\theta}^0$. The corresponding contribution to $P_0(k,\omega)$, say $P_0^\theta(k,\omega)$, under the usual assumptions, with U'(y) approximated by (24) and L again taken as in (25), may be written

$$P_0^\theta(k,\omega) = \rho^2 v_*^3 a^2 I_\theta^2(k,\omega), \quad (37)$$

$$I_\theta(k,\omega) = (kv_*/\omega)\int_0^\delta dy a^{-1}[1+\alpha k_+(a+y)]^{-\frac{1}{2}}(1+y/a)^{-3/2}[\ell n(1+y/a)+C']S_\theta(k_+ y), \quad (37a)$$

where S_θ is related to $-2\hat{T}_{\theta\theta}^0$ as S was to $\hat{T}_{rr}^0 - \hat{T}_{\theta\theta}^0$. In opposite limiting domains, for $a/\delta \ll 1$,

$$I_\theta \sim C'(kv_*/\omega) \times \begin{cases} 1, & k_+ a \gg 1 \\ (k_+ a)^{-3/2}, & k_+ a \gg 1. \end{cases} \quad (38)$$

(If Eq. 32a yields $|C'| \lesssim 1$, in the upper form here C' should be replaced by a coefficient ~1.) Recalling that we are dealing with a formal expansion for $kU_\infty/\omega \ll 1$ (and $k\delta \ll 1$), implying a domain where $\omega = hv_* k_+$, we replace ω accordingly in (38), so that the result conceivably has some applicability in a model encompassing also higher (e.g. convective) values of k. The resulting limiting forms given by (37) for P_0^θ may be subsumed by an assumed interpolation to yield

$$P_0^\theta(k,\omega) \sim C_\theta |C'|^2 \rho^2 v_*^3 a^{-3}(ka)^2 k_+^{-2}[k_+ + (ba)^{-1}]^{-3}, \quad (39)$$

where C_θ is a constant.

6. FURTHER DISCUSSION AND CONCLUSIONS

To reiterate, a decrease in the spectral density of axisymmetric wall pressure with *decreasing* cylinder diameter—ultimately as a^2—is predicted at low dimensionless frequencies and wavenumbers if the pressure in that domain scales on diameter alone (see Eq. 2). In the work here, the likely most plausible scaling together with rough modeling have been introduced to characterize the dominant component of the turbulent field; at relatively small distances from the wall the model spectra conform to the usual principle of local similarity and are otherwise consistent with relevant measurements for cylindrical boundary layers. It is found that for this assumed source scaling the corresponding wall pressure at negligible wave number, at least, indeed scales with cylinder diameter (see Eqs. 26, 27).

At the same time, the predicted rate of decrease with diameter could substantially vanish in some domain of very low frequency and wavenumber if there is even a weak distinct contribution to wall pressure due to a component of the turbulence field that scales rather on boundary-layer thickness [e.g., see the model form (30) or its limit (31)]. There appears no specific present experimental evidence for such a component, but an identifiable field of this character may presumably be present, though weak.

The relative contribution of this component to wall pressure in the low-frequency, low-wavenumber domain naturally depends on its relative source intensity, but also on a factor somewhat like $(\delta/a)^2$ (e.g., see Eq. 31). It may help fix expectations, therefore, to estimate δ/a for given radius a and effective distance x from the transition point upstream. With δ as conventionally defined and $v_*/U = 0.04$ for the flow domain of interest, Eq.A2-7 of Appendix 2, referring to $\delta/a \gg 1$, gives

$$\delta/a = \gamma (x/a)^{2/3} ,$$

where the value of γ (which may depend weakly on Reynolds number) indicated by the measurements of Ref. 19 is $\simeq 0.09$ or by those of Ref. 5 $\simeq 0.13$. For $x/a = 4000$, e.g. $x = 50$m and $2a = 2.5$ cm, assuming $\gamma = 0.12$ yields $\delta/a \simeq 30$. Clearly, then, we will typically be concerned with large values of δ/a such that $10\log(\delta/a)^2$ may be ~ 20.

With regard to the opposite domain of high frequencies but low wavenumbers, the present plausible modeling of the dominant turbulence component leads again to dependence as $a^{-3}v_*^8\omega^{-5}$ (e.g. see Eq. 27). Though it would be extravagant to claim robustness for primitive modeling that entails so many uncertain elements, no definite possible reason for contrary behavior has been uncovered.

Some suggestion of the dependence of wall pressure at non-negligible wavenumbers has been attempted by use of the terms of next order in the formal expansion in terms of boundary-layer sources (see Eq. 32), assuming the same type of model for the dominant turbulent source field. A term proportional to δ/a is obtained but only at wavenumbers so low that the zero-wavenumber part would predominate there (see Eq. 36 with $k_+ \lesssim \delta^{-1}$ and compare Eq. 27). A term is also obtained that differs from the corresponding term $\propto k^2$ in the current model (9a) by a factor $\sim (k_+a)^{-2}$ ($>>1$) at small k_+a (see Eqs. 39, 7).* The formal expansion used, however, nominally requires that $|k|\delta << 1$ as well as $|k|U_\infty/\omega << 1$, so that this modeling of the term of next order in k may be invalid where departure from the zero order is appreciable at all.

---

*The weakly frequency- and wavenumber-dependent factor $\sim|C'|^2$ in (39) (see Eq. 32a) is also a new feature that will persist in the corresponding contribution more generally.

In view of this latter limitation it seems useful for further semiempirical modeling to seek the formal expansion to the subject order where the condition $|k|\delta<<1$ is relaxed (but still $|k|U_\infty/\omega<<1$). The corresponding generalization was carried out in Ref. 3, Eq. 35, in the instance of planar, incompressible flow. In further work the same may be attempted for the axisymmetric component in incompressible cylindrical flow.*

APPENDIX 1. INDICATIVE MODELING OF TURBULENCE SPECTRA IN CYLINDRICAL COORDINATES

As suggested in Sec. 4, and underlying modeling pursued there, model spectra are constructed here in cylindrical coordinates without explicit reference to a cylindrical wall as the physical generator of the turbulence. Consider first a cross-spectrum $E(r,r',\phi,k,\omega)$ between amplitudes of a quantity for axial (x) wavenumber k and frequency ω, evaluated at position vectors $\underline{r},\underline{r}'$ in the plane normal to x with polar coordinates (r,θ), $(r',\theta+\phi)$. The random process assumed is statistically axisymmetric in the normal plane, so that E in fact depends on the angular coordinates only via their difference (see sketch). E may be decomposed into angular harmonics,

$$E(r,r',\phi,k,\omega) = \sum_{m=-\infty}^{\infty} e^{im\phi} E_m(r,r',k,\omega), \qquad \text{(A1-1a)}$$

$$E_m(r,r',k,\omega) = (2\pi)^{-1} \int_{-\pi}^{\pi} d\phi e^{-im\phi} E(r,r',\phi,k,\omega). \qquad \text{(A1-1b)}$$

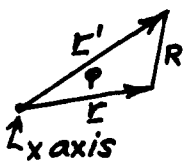

*By analogy with the planar result, it is expected that the thus generalized form of Eq. 32 will involve a factor in the integrand that decreases with ky.

Suppose initially that the process is homogeneous and isotropic in the normal plane; then the dependence of E may also be expressed by

$$E(r,r',\phi,k,\omega) = E(R(\phi),k,\omega),$$
$$R(\phi) \equiv |\underline{r}'-\underline{r}| = (r^2+r'^2-2rr'\cos\phi)^{\frac{1}{2}} \qquad \text{(A1-2)}$$

For representative modeling, as discussed in the text, suppose that E depends on k and ω only via k_+, defined in Eq. 7, and on a single length scale Δ and velocity scale v_*. For definiteness, consider the cross-spectrum of the axial component of fluctuating velocity: $E \equiv E_{11}$, say.* Then

$$E_{11}(r,r',\phi,k,\omega) = E_{11}(R(\phi),k,\omega) = v_*\Delta^2 F_{11}(k_+\Delta,R(\phi)/\Delta), \qquad \text{(A1-3)}$$

where F_{11} is a dimensionless function of the given arguments.

By Fourier transformation of E_{11} also over the coordinates of separation in the normal plane, a four-dimensional spectral density may be defined that depends on the three-dimensional wavevector $\underline{k}$ only via its axial and normal components k and K, say. This spectral density is then expressed inversely, using (A1-3), by

$$E_{11}(k,K,\omega) = (2\pi)^{-2}(2\pi)\int_0^\infty dRRJ_0(KR)E_{11}(R,k,\omega)$$
$$= v_*\Delta^4 G_{11}(K\Delta,k_+\Delta),$$
$$G_{11}(K\Delta,k_+\Delta) = (2\pi)^{-1}\int_0^\infty dzzJ_0(K\Delta z)F_{11}(k_+\Delta,z) \; . \qquad \text{(A1-4)}$$

*It would be expected that the spectral density of one component or function of velocity may be more nearly a function of k_+ than another and that the value of the velocity scale factor h in Eq. 7 for k_+ that renders this most nearly true will also depend on the identity of the component or function (cf. Ref. 21, Sec. 2.3).

F_{11} and G_{11} in Eqs. A1-3 and A1-4 may be related to the corresponding space-time correlation, which under present assumptions may be written, for axial separation x, normal separation R, and time delay τ,

$$W_{11}(x,R,\tau) = v_*^2 f(x_+/\Delta, R/\Delta),$$
$$x_+ = [(x-u_c\tau)^2+(hv_*\tau)^2]^{\frac{1}{2}} ; \qquad \text{(A1-5)}$$

explicitly,

$$F_{11}(k_+\Delta, R/\Delta) = (2\pi)^{-1}h^{-1}\int_0^\infty dz z J_0(k_+\Delta z) f(z,R/\Delta),$$
$$G_{11}(K\Delta,k_+\Delta) = (2\pi)^{-2}h^{-1}\int_0^\infty dz z J_0(k_+\Delta z)\int_0^\infty d\zeta\zeta J_0(K\Delta\zeta) f(z,\zeta). \qquad \text{(A1-6)}$$

Likewise, for representative modeling suppose that in the spatial correlation function the axial and normal components of separation add in quadrature; then (A1-5) assumes the still more special form

$$W_{11}(x,R,\tau) = v_*^2 f(r_+/\Delta), \qquad \text{(A1-7)}$$
$$r_+ = [(x-u_c\tau)^2+(\beta R)^2+(hv_*\tau)^2]^{\frac{1}{2}} , \quad (\beta = \text{const.})$$

and the dimensionless four-spectrum G_{11} of (A1-4) assumes the dual form

$$G_{11}(K_+\Delta) = (2\pi)^{-2}(h\beta)^{-1}\int_0^\infty ds s^3 (K_+\Delta s)^{-1} J_1(K_+\Delta s) f(s),$$
$$K_+ = (k_+^2+\beta^{-2}K^2)^{\frac{1}{2}} = [(\omega-u_c k)^2/(hv_*)^2+k^2+\beta^{-2}K^2]^{\frac{1}{2}} . \qquad \text{(A1-8)}$$

A convenient class of such correlations and spectra that, by variation of its parameters (A_0, b_0, b_1, ν), encompasses a broad range of plausible functional behavior is defined by assuming in (A1-7) that

$$f(\rho) = A_0(\rho^2+b_1^2)^{-\nu/2}K_\nu(b_0(\rho^2+c_1^2)^{\frac{1}{2}}) \quad . \qquad \text{(A1-9)}$$

Performing the required transforms by Ref. 22, p. 72, (35) yields for corresponding spectra (see Eqs. A1-3, A1-4)

$$F_{11}(k_+\Delta,R/\Delta) = (2\pi)^{-1}A_0h^{-1}b_0^{-\nu}(\beta^2R^2/\Delta^2+b_1^2)^{(1-\nu)/2}(k_+^2\Delta^2+b_0^2)^{(\nu-1)/2}$$
$$\times K_{\nu-1}((\beta^2R^2/\Delta^2+b_1^2)^{\frac{1}{2}}(k_+^2\Delta^2+b_0^2)^{\frac{1}{2}}) \quad , \qquad \text{(A1-10)}$$

$$G_{11}(K_+\Delta) = (2\pi)^{-2}A_0h^{-1}\beta^{-2}b_0^{-\nu}b_1^{2-\nu}(K_+^2\Delta^2+b_0^2)^{-1+\nu/2}K_{\nu-2}(b_1(K_+^2\Delta^2+b_0^2)^{\frac{1}{2}}) \, . \qquad \text{(A1-11)}$$

It is recalled that $K_{-\nu}(z) = K_\nu(z)$; thus the class of functions (A1-11) for the four-spectrum is the same as the class (A1-9) for the space-time correlation. This is the same class of functions introduced in Ref. 11, Eq. 36.

For $b_1 \to 0$, the spectral dependence (A1-11) becomes power-law:

$$G_{11} \propto (K_+^2\Delta^2+b_0^2)^{-(2-\nu)} \quad .$$

If also $\nu = 0$, it is noted, the result (A1-4) for E_{11} when $K_+\Delta >> b_0$ becomes scale-independent, i.e. the dependence on Δ cancels.

To achieve the fit to the experimental results of Ref. 18 discussed in Ref. 11, p. 43, referring to a planar wall,* with the present scale Δ taken proportional there to $\xi \equiv (yy')^{\frac{1}{2}}$, by inspection of Eqs. 40, 36, and the choice $\nu = 1$ there, the corresponding assumption here is $\nu = 1$. Other parameters of that fit imply also that $b_0 = 0$ and $b_1\Delta = (2yy')^{\frac{1}{2}}$ (in the planar limit).

*The fit to this experiment, as noted in Ref. 11, does not involve the (weak) temporal dependence in the convected frame nor hence validate the modeling assumption of space-time isotropy (within a scale factor).

The choice of a similar model for the cylindrical case was introduced following Eq. 17 of the text. The present choice of parameters will be referred to here as the "standard model."

The models considered in this appendix implicitly assume the scale Δ to be independent of the spatial points involved in the correlation referred to. In the actual instance of wall turbulence, as discussed in the text, dependence of Δ on y,y' is simply assumed afterward in the definition of the intended model from the formally constructed one, as implied in the preceding paragraph.

For the above standard model, the cross-spectrum (A1-3) has the form

$$E_{11}(r,r',\phi,k,\omega) = A'v_*\Delta^2 K_0(k_+(\beta^2R^2+b_1^2\Delta^2)^{\frac{1}{2}}). \qquad \text{(A1-12)}$$

We proceed by rough approximations to simplify the form of the model as used in the text and to explore its characteristics. By Eq. A1-1b the m-th harmonic cross-spectral component, $E^m_{11}(r,r',k,\omega)$, is given by

$$E^m_{11}(r,r',k,\omega) = (2\pi)^{-1}A'v_*\Delta^2\int_{-\pi}^{\pi} d\phi e^{-im\phi}K_0(k_+(\beta^2R^2(\phi)+b_1^2\Delta^2)^{\frac{1}{2}}) \qquad \text{(A1-13)}$$

with $R(\phi)$ as in (A1-2).

For $r=r'$, one has $R(\phi) = 2r\left|\sin\frac{1}{2}\phi\right|$. For r,r' not necessarily equal but $\phi \lesssim 1$, one has roughly

$$R(\phi) \sim [(r'-r)^2+rr'\phi^2]^{\frac{1}{2}} ; \qquad \text{(A1-14)}$$

in the most contrary case where the two points are diametrically opposed ($\phi=\pi$), this yields

$$R(\phi) \sim (r'+r)^2+(\pi^2-4)rr' ,$$

while the exact result is $R(\pi) = (r'+r)^2$. For indicative, order-of-magnitude scaling estimates, as in the text, it appears that approximation (A1-14) will suffice.

Eqs. A1-13 and A1-14 yield for the axisymmetric harmonic m=0

$$E_{11}^0(r,r',k,\omega) \simeq \pi^{-1}A'v_*\Delta^2 I_0,$$

$$I_0 = \int_0^\pi d\phi K_0(k_+(\Delta_r^2+\beta^2 rr'\phi^2)^{\frac{1}{2}}),$$

$$\Delta_r^2 \equiv \beta^2(r'-r)^2+b_1^2\Delta^2.$$

By use of limiting forms of $K_0(z)$ for small and large arguments, I_0 can be estimated in pertinent distinct domains. In an approximation where $\ell n[k_+\beta(rr')^{\frac{1}{2}}]$ is not distinguished from a constant, the result may be written simply as

$$E_{11}^0(r,r',k,\omega) \sim v_*\Delta^2 \times \begin{cases} 1, & k_+\Delta_r \lesssim 1, k_+(rr')^{\frac{1}{2}}\pi\beta \lesssim 1 \\ [k_+(rr')^{\frac{1}{2}}\beta]^{-1}, & k_+\Delta_r \lesssim 1, k_+(rr')^{\frac{1}{2}}\pi\beta \gtrsim 1 \\ [k_+(rr')^{\frac{1}{2}}\beta]^{-1}\exp(-k_+\Delta_r), & k_+\Delta_r \gtrsim 1 \end{cases} \quad \text{(A1-15)}$$

This estimate underlies and exemplifies form (15)' in the text.

Referring for a moment to arbitrary harmonics m, it may be expected from Eq. A1-1b or A1-13 that $E_{11}^m(r,r',k,\omega)$ will remain substantial relative to the value for m=0 for $|m| \lesssim 1/\Delta\phi$, where $\Delta\phi$ is the halfwidth in ϕ over which $E_{11}(r,r',\phi,k,\omega)$ remains relatively appreciable. Hence the point spectrum (r'=r) is estimated by

$$E_{11}(r,k,\omega) = \sum_m E_{11}^m(r,r,k,\omega) \sim ME_{11}^0(r,r,k,\omega),$$

$$M = \begin{cases} 1, & \Delta\phi \gtrsim 1 \\ 2/\Delta\phi+1, & \Delta\phi \lesssim 1. \end{cases}$$

For the standard model (A1-12), with r'=r, one has $\Delta\phi \sim b_1\Delta/\beta r$.

We consider now briefly, in place of the standard model, one where in (A1-9)-(A1-11) $b_1 \to 0$ and $\mu \equiv 1-\nu > 0$. By (A1-10)

$$E_{11}(r,r',\phi,k,\omega) + Bv_*\Delta^2(\beta R/\Delta)^{\mu}(k_+^2\Delta^2+b_0^2)^{-\mu/2}K_{\mu}((k_+^2\Delta^2+b_0^2)^{\frac{1}{2}}\beta R/\Delta). \tag{A1-16}$$

In this case, in place of estimate (A1-15) one obtains

$$E_{11}^{0}(r,r',k,\omega) \sim v_*\Delta^2(k_\Delta\Delta)^{-2\mu}\times \begin{cases} 1, & k_\Delta|r'-r|\beta\lesssim 1,\ k_\Delta(rr')^{\frac{1}{2}}\pi\beta\lesssim 1 \\ [k_\Delta(rr')^{\frac{1}{2}}\beta]^{-1}, & k_\Delta|r'-r|\beta\lesssim 1,\ k_\Delta(rr')^{\frac{1}{2}}\pi\beta\gtrsim 1 \\ [k_\Delta(rr')^{\frac{1}{2}}\beta]^{-1}[k_\Delta|r'-r|\beta]^{\mu}\exp(-\beta k_\Delta|r'-r|), & k_\Delta|r'-r|\beta\gtrsim 1 \end{cases} \tag{A1-17}$$

where $k_\Delta = (k_+^2+b_0^2\Delta^{-2})^{\frac{1}{2}}$. The halfwidth, for r'=r, is given by $\Delta\phi \sim 1/\beta k_\Delta r$.

Estimates (A1-15) and (A1-17) can be subsumed in an expression valid for the class of functions (A1-9)-(A1-11) more generally.

APPENDIX 2. MEAN VELOCITY PROFILE AND BOUNDARY-LAYER GROWTH IN TURBULENT FLOW ALONG A CYLINDER: COMPARISONS WITH RECENT MEASUREMENTS

A.2.1 Mean velocity profile

Reference was made in this memo to the dependence of a mixing length derived for the "logarithmic range" of Rao's preseciption[20] for the mean velocity in flow along a cylinder. For possible future reference as well, we therefore append a comparison of a result of this prescription with the mean profiles measured by Willmarth *et al.*[19] on cylinders of various radii and by Leehey and Stellinger[5] on a (thin) cylinder at various streamwise positions. These measurements are much more extensive than the earlier ones by Richmond[25] compared in this way previously.[26]

The Rao prescription is reviewed as follows. The mean velocity profile $U(x,y)$ in the turbulent flow (without pressure gradient) may be written, over some inner range of wall distances y (limited at least by the condition $y \lesssim \delta$), in the functional form

$$U/v_* = F(v_* y/\nu, y/a) \qquad \text{(A2-1)}$$

(where v_* may depend on x). Rao's hypothesis prescribes the function F for the cylinder in terms of its limiting form, $F(v_* y/\nu, 0)$, for a planar boundary:

$$F(v_* y/\nu, y/a) = F((v_* a/\nu)\ell n(1+y/a), 0). \qquad \text{(A2-2)}$$

Within the viscous sublayer where $F(v_* y/\nu, 0) = v_* y/\nu$, this prescription yields

$$U/v_* = (v_* a/\nu)\ell n(1+y/a),$$

which, apart from terms of the order of $(y/a)^4$, correctly represents the result for a laminar cylindrical boundary layer and for the viscous sublayer of the subject turbulent one. Outside this domain (i.e., for $v_* y/\nu \gtrsim 6$ or $y/a \gtrsim 1$), prescription (A2-2) apparently lacks any sustainable basis except as a plausible semiempirical trial form.[27]

As in Ref. 26, we apply (A2-2) numerically here on assumption that the profile $F(y_+, 0)$ for a planar boundary is adequately approximated by use of Squire's transitional profile and without regard to changing dependence in the outer wake-like region where $y \sim \delta$:

$$F(y_+,0) = \begin{cases} y_+ , & 0<y_+<7.4 \\ 2.5\ell n(y_+-4.9)+5.1, & y_+>7.4 \end{cases} \qquad \text{(A2-3)}$$

Results of Eqs. A2-1 to A2-3 are compared in Fig. A2-1 with representative velocity profiles measured by Willmarth *et al.*[19] on cylinders of various radii 0.01 in. to 1 in., as given in their Fig. 32. The assumed profile of Eq. A2-3 for planar boundary is also shown along with that of Coles[28] as given in Ref. 19. The computed profiles are seen to provide a fair representation of the data. More specifically, the fit is excellent for all v_*y/ν (even such that $y/a>>1$) at $\delta/a \simeq 16$ (with $v_*a/\nu \sim 200$), apart from apparent inexactitude of the assumed form (A2-3) in the transitional region. The measured dependence on δ/a or on v_*a/ν at fixed v_*y/ν, however, where $5 \lesssim \delta/a \lesssim 27$, is greater than that computed.

Computed results are similarly compared with profiles measured by Leehey and Stellinger[5] in Figs. 2 to 4, as given in their identically numbered figures. The data in each figure refer to a fixed free-stream speed and hence roughly equal values of v_*a/ν but to a wide range of distances x along the cylinder and hence also of δ/a. The computed curve shown in each figure corresponds to choice of the smallest of the pertinent series of values of v_*a/ν quoted by the authors, but for the spread of values of v_*a/ν in each instance the range of variation of U/v_* at fixed v_*y/ν is negligible—only about 0.2 at the greatest values of v_*y/ν and less at smaller. The assumed profile (A2-3) for a planar boundary is again shown in Fig. 2 and in Figs. 2 to 4 of the Coles profile as given in Ref. 5.

The measured results display substantial dependence on δ/a, especially at the largest v_*a/ν, extending in this case even into the range where $y/a \lesssim 1$. The calculated results in each figure agree

very well with the measured profiles for $\delta/a \sim 15$ to 20. For the assumed δ-independent planar profile (A2-3), however, the computed profiles do not depend on δ (at fixed v_*a/ν) and do not capture the decrease with δ/a displayed (at fixed v_*y/ν) by the measured profiles. This dependence on δ/a was emphasized and discussed under a different assumption by Leehey and Stellinger.[5] The sense and magnitude of the discrepancy at larger δ/a parallels that noted above in Fig. 1 in the instance of the measurements of Ref. 19. (See also Ref. 30.)

The Rao hypothesis, in summary, seems to provide a useful rough description of the mean velocity profile on cylinders but does not encompass the full dependence on the characterizing variables δ/a and v_*a/ν. This limitation, moreover, would not be removed by including the dependence on the outer variable y/δ in Eq. A2-2 as it enters the profile for a planar boundary.

As a matter merely of curve-fitting, on the basis of Figs. 1 to 4 a good approximation to mean profiles outside the transition layer is obtainable by retaining Eq. A2-2 but adjoining to F in Eq. A2-1 a factor $M(\delta/a)$, say, where $M(0) = 1$ and where $M(\delta/a)$ increases sharply to a broad maximum of about 1.1 for $\delta/a \sim 5$ to 9, returns through the value 1 again at about $\delta/a = 18$, and decreases to about 0.85 for $\delta/a \sim 27$ to 48. (Cf. Ref. 5, Eq. 9.) To retain a good approximation in the transition and sublayers, however, since the required correction tends to unity there, one would need to let $M(\delta/a)$ depend also on v_*y/ν for $v_*y/\nu \lesssim 25$.

A factor $M(\delta/a)$ independent of y outside the transition layer, it is noted, would imply a corresponding correction factor $1/M(\delta/a)$ in the mixing length inferred from Rao's hypothesis (Eq. 25).

A.2.2 Boundary-layer growth

A simple, rudimentary account of growth of the turbulent boundary layer on a cylinder can be given in the approximation, closely correct for the parameter domain of concern for towed arrays, where the wall friction velocity v_* is independent of distance x. The resulting form may then be appraised by comparison with measurements of δ by Willmarth *et al.*[19] and by Leehey and Stellinger,[5] where δ is defined by the condition $U(x,\delta) = 0.99U_\infty$.

First, $d\delta/dx$ is of the order of the ratio of the normal (y) velocity to U_∞ at the edge of the layer, i.e. the boundary of the streamlines of rotational motion. By similarity considerations (see R. E. Kronauer, Ref. 6), this normal component will be nearly proportional to the rms fluctuating streamwise component. By measurements of Leehey and Stellinger, discussed by Kronauer[6] and referred to in the above text, the latter component, for wall distances outside the transition layer out nearly to $y=\delta$ varies as $v_*(a/r)^{1/2}$. Accordingly, we have

$$d\delta/dx = D(v_*/U_\infty)a^{1/2}/(a+\delta)^{1/2} , \qquad \text{(A2-5)}$$

where D is a numerical constant. Integration of (A2-5) from a virtual origin x=0 (defined by extrapolation to $\delta=0$) yields

$$\delta/a = [1+(3/2)D(v_*/U_\infty)x/a]^{2/3}-1 . \qquad \text{(A2-6)}$$

In opposite limits this becomes

$$\begin{aligned} \delta/a &\to [(3D/2)(v_*/U_\infty)x/a]^{2/3} , \quad \delta/a \gg 1 \\ \delta &\to Dv_*/U_\infty , \quad \delta/a \ll 1 \end{aligned} \qquad \text{(A2-7)}$$

(but, contrary to our assumption, v_* is not so nearly constant in the latter, planar limit).

A second, perhaps less convincing approach to this result is based on considering, as in the treatment of drag on wake-generating bodies (e.g., see Ref. 29, Secs. 21, 36), the transport of momentum through a closed surface surrounding the cylinder. This surface may be conceived so that the only nonvanishing contribution arises from flux through a circular area $\pi(a+\delta)^2$ of a normal plane drawn somewhat aft of the real or imagined aft terminus of the cylinder. With friction velocity still approximated as constant over the length x of the cylinder upstream of this plane, conservation of momentum implies an equation for drag:

$$2\pi a x \rho v_*^2 = -\rho U_\infty \cdot 2\pi \int_0^{a+\delta} dr r u_{av}(r) \ , \qquad \text{(A2-8)}$$

where $u_{av}(r)$ denotes the mean downstream component of fluid velocity relative to the free stream (thus $u_{av}<0$). Suppose that just downstream of the terminus this incremental velocity profile due to the dragging of fluid by the wall of the cylinder upstream is nearly proportional to that of the rms fluctuating velocity components at the terminus, i.e. $u_{av}=-Cv_*(a/r)^{\frac{1}{2}}$ for $a<r<a+\delta$, where C is a constant. Then Eq. (A2-8) becomes

$$2\pi a x \rho v_*^2 = 2\pi \rho v_* U_\infty C \int_a^{a+\delta} dr r (a/r)^{\frac{1}{2}} \ ;$$

integration yields again just the result (A2-6) provided that $C=D^{-1}$.

To check (A2-6) or (A2-7) against measured results and infer a rough value for D, one may form (in the instance of Eq. (A2-7) for $\delta/a>>1$) the ratio $(\delta/a)/[(v_*/U_\infty)(x/a)]^{2/3}$ for the various data sets of Refs. 5 and 19 and see if it is nearly constant (or at least has no substantial systematic variation). For the 14 data sets of Ref. 19, Table 1, excluding two (3 and 12) rejected as out of line with the remaining ones, the inferred value of the cited ratio varies by less than a factor two (not monotonically with δ/a) while the range of hose diameters encompasses a factor 100. The mean value inferred for D is about 0.45. Similarly, for

the 23 possible data sets of Ref. 5, Table 1, accepting the value of v_* therein obtained by fitting velocity profiles in the buffer layer, the cited ratio varies by a factor of about two while the range of positions x is 10.5. The mean value inferred for D in this case is about 0.8. The corresponding value C = 1.25 yields a result that $u_{av} \simeq -u$ (at wall distances where $u \propto r^{-\frac{1}{2}}$), where u is the measured rms streamwise velocity component, as seen in Fig. 2.3-6 of Ref. 6 (based on Fig. 3 of Ref. 5).

REFERENCES

1. D. M. Chase, "Modeling the wavenumber-frequency spectral density of wall pressure in turbulent flow along a cylinder," CI Tech Memo No. 9, 7 December 1979.

2. D. M. Chase, "Implications of recent high-speed trials of towed array modules for the spectral density of turbulent wall pressure,"(U), CI Tech Memo No. 12, 18 April 1980 (Conf.).

3. D. M. Chase and C. F. Noiseux, "Turbulent wall pressure at low wavenumbers: relation to nonlinear sources in planar and cylindrical flow," CI Tech Memo No. 18, 30 March 1981.

4. D. M. Chase, "Towed-array self noise: Description and projection from the perspective of analytical modeling"(U), paper presented at 33rd Navy Symposium on Underwater Acoustics, Part III, 1323-1338, December 1979 (Conf.).

5. P. Leehey and T. S. Stellinger, Jr., "A wake law for an axially symmetric turbulent boundary layer on a cylinder," MIT, Dept. of Ocean Engineering, unpublished, January 1978.

6. R. E. Kronauer, Sec. 2.3 in "Design principles for towed arrays"(U), NSEA Code 63R, Feb. 1980 (Conf.).

7. P. Bradshaw, "'Inactive' motion and pressure fluctuations in turbulent boundary layers," *J. Fluid Mech. 30*, 241-258 (1967).

8. A. A. Townsend, *J. Fluid Mech. 11*, 97 (1961).

9. D. M. Chase, "Turbulence-induced noise in fluid-filled towed arrays"(U), BBN Report No. 3773, March 1978 (Conf.).

10. D. M. Chase, "Modeling of turbulent wall-pressure spectra on towed cylinders," BBN Tech Memo No. 352, May 1977.

11. D. M. Chase, "Modeling the wavevector-frequency spectrum of turbulent-boundary-layer wall pressure," *J. Sound Vib., 70*, 29-67 (1980).

12. P. W. Jameson, "Measurement of the low-wavenumber component of turbulent boundary layer pressure spectral density," Proc. Symposium on Turbulence in Liquids, Univ. of Missouri, Rolla, 192-200 (1975).

13. D. M. Chase, "Modeling analysis of noise levels in recent NUSC towed-array modules"(U), CI Tech Memo No. 11 17 March 1980 (Conf.).

14. A. E. Markowitz, "Turbulent boundary layer wall pressure fluctuation and wall acceleration measurements on a long flexible wall cylinder towed at sea," NUSC Tech. Rept. 5305, August 1976.

15. D. M. Chase, "Modeling of turbulent pressure on a towed-array hose in the convective domain on the basis of recent measurements," BBN Tech Memo No. 335, February 1977.

16. D. M. Chase, "Wall pressure fluctuations on towed cylinders," BBN Tech Memo No. 189, April 1974.

17. W.R.B. Morrison and R. E. Kronauer, "Structural similarity for fully developed turbulence in smooth tubes," *J. Fluid Mech. 39*, 117-141 (1969).

18. W. Morrison, K. Bullock, and F. Abernathy, "Structural similarity in radial correlations and spectra of longitudinal velocity fluctuations in pipe flow," *J. Fluid Mech. 88*, 585-608 (1978).

19. W. W. Willmarth, *et al.*, "Axially symmetric turbulent boundary layers on cylinders: mean velocity profiles and wall pressure fluctuations," Univ. of Michigan, Dept. of Aerospace Engineering, 021490-3-T, June 1975; *J. Fluid Mech. 76*, 35-64 (1976).

20. G.N.V. Rao, "The law of the wall in a thick axisymmetric turbulent boundary layer," *J. Appl. Mech., Transactions of the ASME, 34,* 237-238 (1967).

21. D. M. Chase, "Space-time correlations of velocity and pressure and the role of convection for homogeneous turbulence in the universal range," *Acustica 22,* 303-320 (1969/70).

22. H. Bateman, *Tables of integral transforms,* Vol. 2, McGraw-Hill, New York, 1954.

23. J. F. Waters, "ONR high-speed towed array sea trial 9A10 quick-look data report"(U), MAR, Inc., Tech. Rept. 234, Jan. 1980 (Conf.).

24. Data from sea trial 9A10 supplied to Chase Inc. by NUSC/NLL; see also R. O. Hauptmann and J. S. Diggs, "Results of towed array exploratory development high-speed sea test (9A10) of FY80"(U), NUSC/NLL TM 801053, November 1980 (Conf.).

25. R. L. Richmond, "Experimental investigation of thick axially symmetric boundary layers on cylinders at subsonic and supersonic speeds," CIT, Guggenheim Aero. Lab., Pasadena, Hypersonic Research Project Memo 39, June 1957.

26. D. M. Chase, "Mean velocity profile of a thick turbulent boundary layer," *AIAA J. 10,* 849-850 (1972); "Reply by author to P. Bradshaw and V. C. Patel," *AIAA J. 11,*894-895 (1973).

27. P. Bradshaw and V. C. Patel, "Comment on 'Mean velocity profile of a thick turbulent boundary layer along a circular cylinder,'" *AIAA J. 11,* 893-894 (1973).

28. D. E. Coles, "The law of the wall in turbulent shear flow," *50 Jahre Grenzschichtforschung,* F. Vieweg und Sohn, Braunschweig, 153 (1955).

29. L. D. Landau and E. M. Lifshitz, *Fluid mechanics,* Addison-Wesley, Reading, 1959.

30. N. Afzal and R. Narasimha, "Axisymmetric turbulent boundary layer along a circular cylinder at constant pressure," *J. Fluid Mech. 74,* 113-128 (1976).

CAPTIONS FOR FIGURES

1. Root-mean-squared longitudinal component of turbulent velocity vs wall distance for thick layer on cylinder (from Ref. 6, Fig. 2.3-6, based on Ref. 5, Fig. 8).

A2-1. Measured and computed mean velocity profiles for cylinders of different diameters. Measured: Fig. 32 of Ref. 19; computed: Eqs. A2-1 to A2-3 with av_*/ν from Ref. 19, Table 1, tabulated below (and planar limit $av_*/\nu=\infty$); also, Coles' profile for planar flow from Ref. 19, Fig. 32.

Symbol	δ/a	av_*/ν
◓	1.8	2710
▲	4.1	1360
△	4.7	751
■	9.4	389
□	16.0	198
●	27.0	83.3
○	37.5	46.1

A2-2. Measured and computed mean velocity profiles for a cylinder at different longitudinal positions. Measured: Fig. 2 of Ref. 5 (see table below); computed: Eqs. A2-1 to A2-3 for $av_*/\nu = 57.9$ (and for planar limit $av_*/\nu=_\infty$); also, Cole's profile for planar flow from Ref. 5, Fig. 2).

Symbol	δ/a	av_*/ν
▲	25.5	57.9
△	26.4	59.1
■	25.6	59.9
□	28.1	58.7
●	29.2	59.8
○	41.4	61.3

CAPTIONS FOR FIGURES (Cont'd.)

A2-3. Profiles as in Fig. A2-2 but from Fig. 3 of Ref. 5 for parameters tabulated below, and computed profile for $av_*/\nu = 81.9$

Symbol	X	◐	⊠	⊖	▲	△	■	●	○
δ/a	15.3	20.0	17.3	24.5	26.8	29.0	31.4	44.1	38.4
av_*/ν	83.3	81.9	83.4	83.4	84.1	85.7	86.9	88.1	90.6

A2-4 Profiles as in Fig. A2-2 but from Fig. 4 of Ref. 5 for parameters tabulated below, and computed profile for $av_*/\nu = 102.8$.

Symbol	◐	⊠	⊖	▲	△	■	□	○
δ/a	18.3	16.3	23.3	27.4	26.0	24.5	45.4	47.5
av_*/ν	103.2	102.8	105.3	108.1	116.2	117.3	115.0	115.0

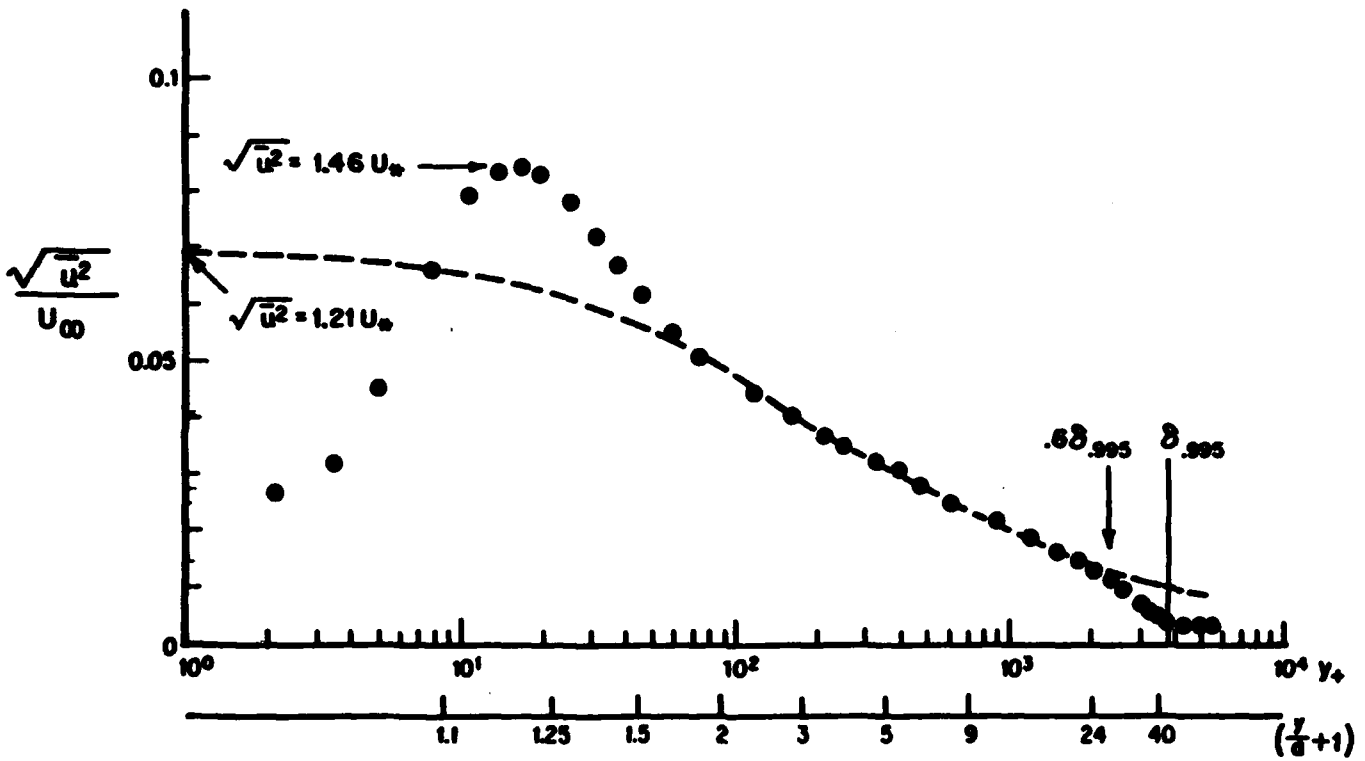
0.1
0.05
0
$\frac{\sqrt{\overline{u^2}}}{U_\infty}$
$\sqrt{\overline{u^2}} = 1.46\,U_\tau$
$\sqrt{\overline{u^2}} = 1.21\,U_\tau$
$.6\delta_{.995}$
$\delta_{.995}$
10^0
10^1
10^2
10^3
10^4 y_+
1.1
1.25
1.5
2
3
5
9
24
40
$(\frac{y}{\delta}+1)$

Fig. 1

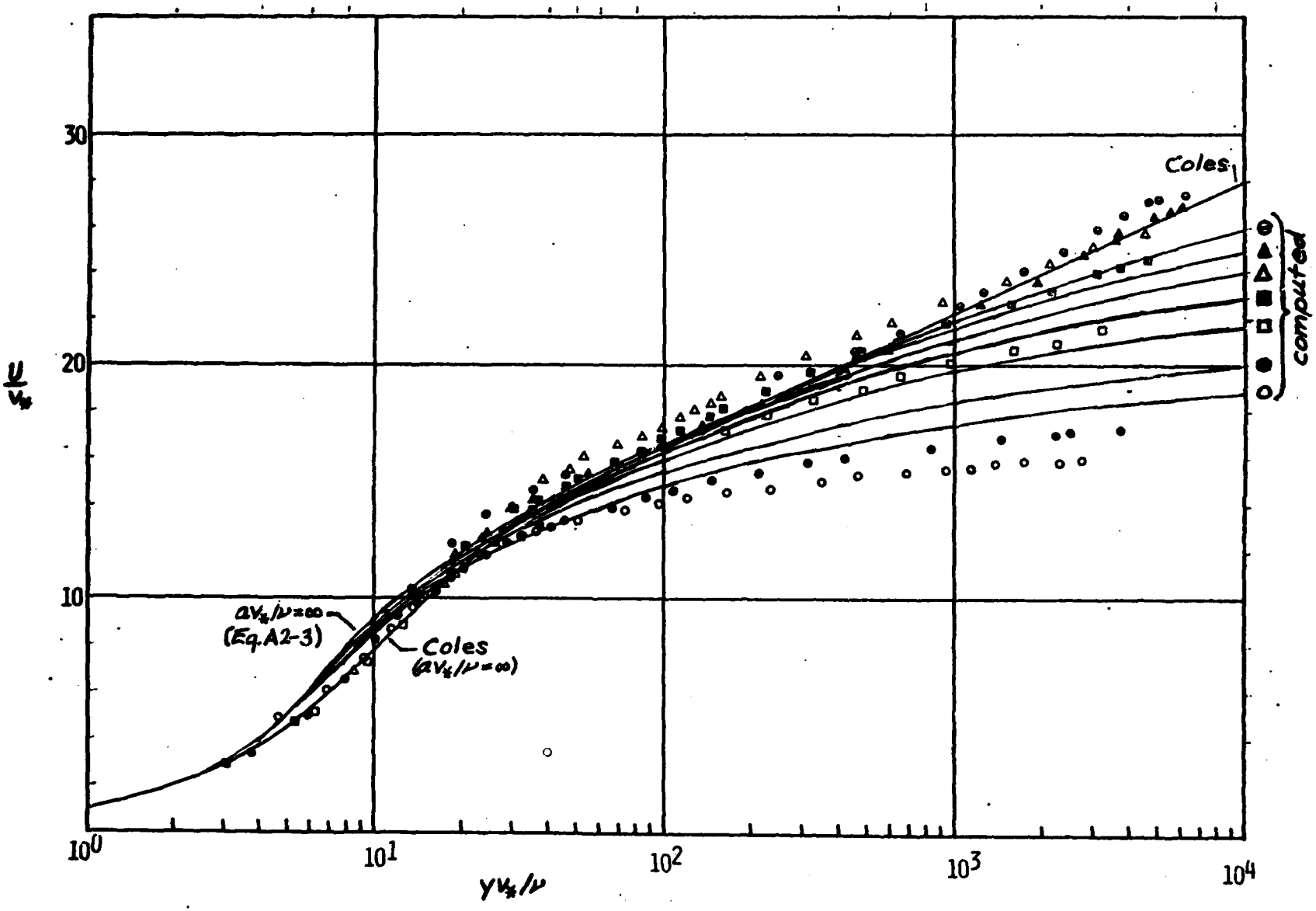
30
20
10
10^0
10^1
10^2
10^3
10^4
$\frac{u}{v_*}$
yv_*/ν
Coles
computed
$av_*/\nu=\infty$
(Eq. A2-3)
Coles
($av_*/\nu=\infty$)

Fig. A2-1

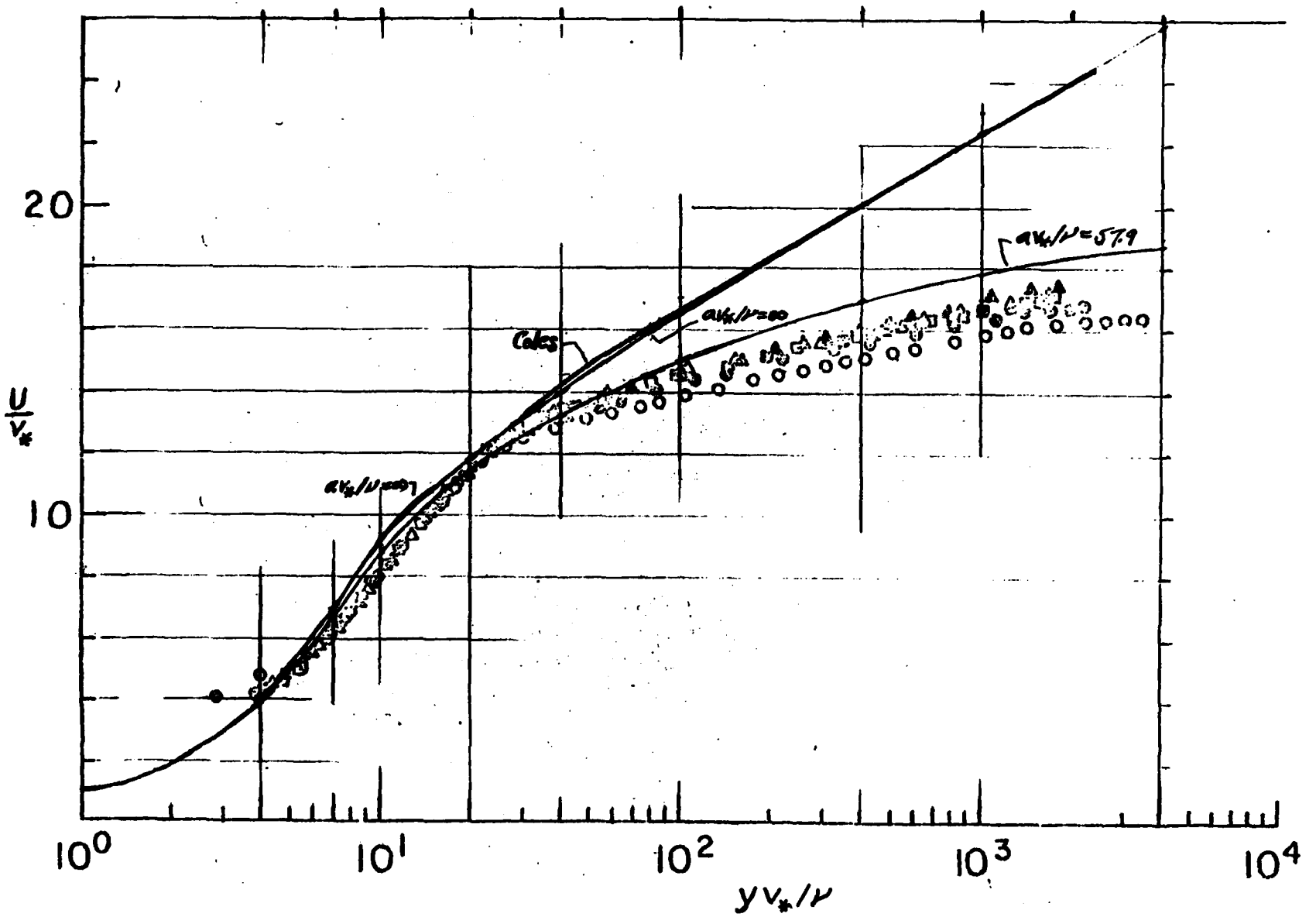
20
10
$\frac{U}{v_*}$
$aV_*/\nu = 57.9$
$aV_*/\nu = \infty$
Coles
$aV_*/\nu = 0$
10^0
10^1
10^2
10^3
10^4
yV_*/ν

Figure A2-2

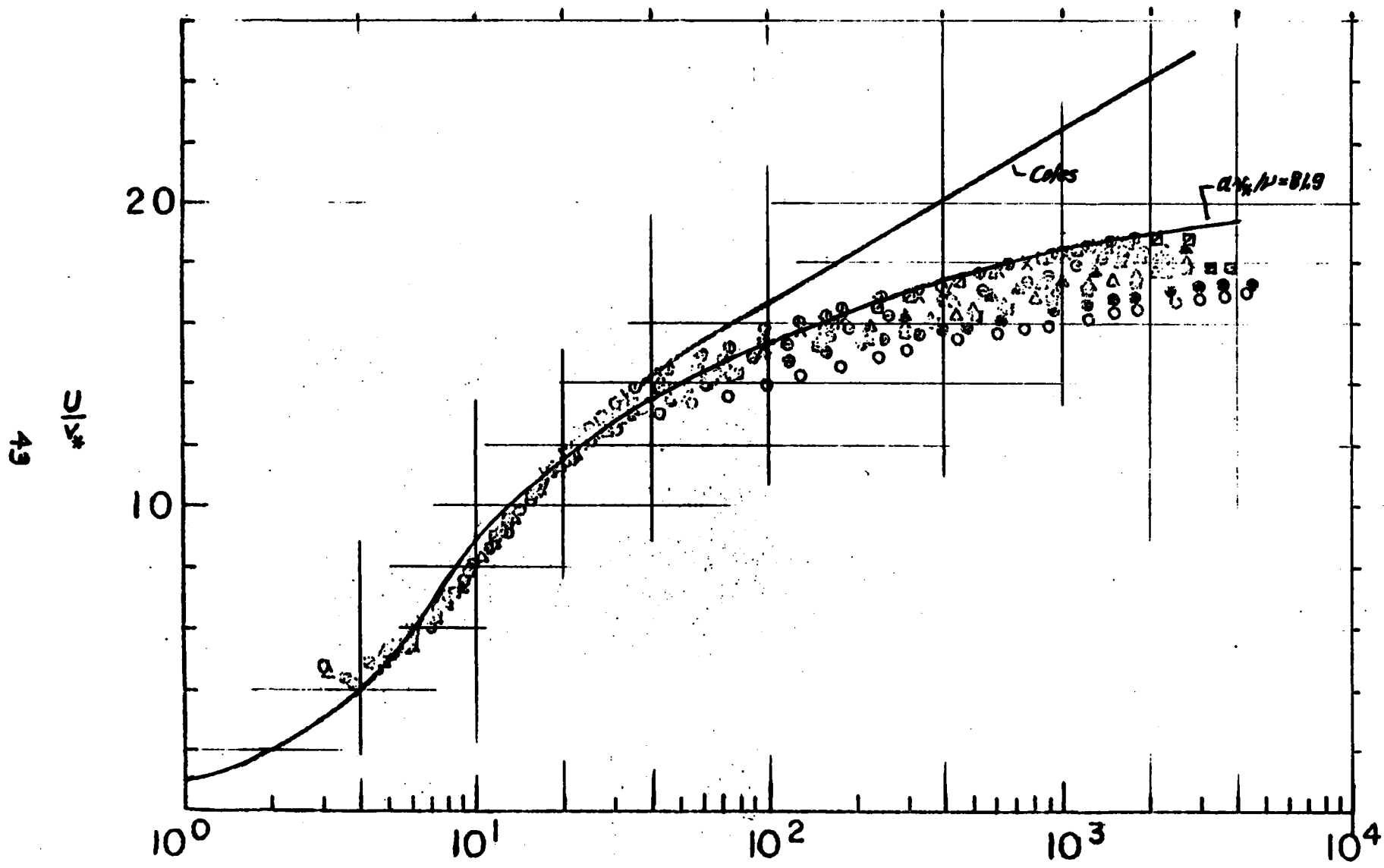

Figure A2-3

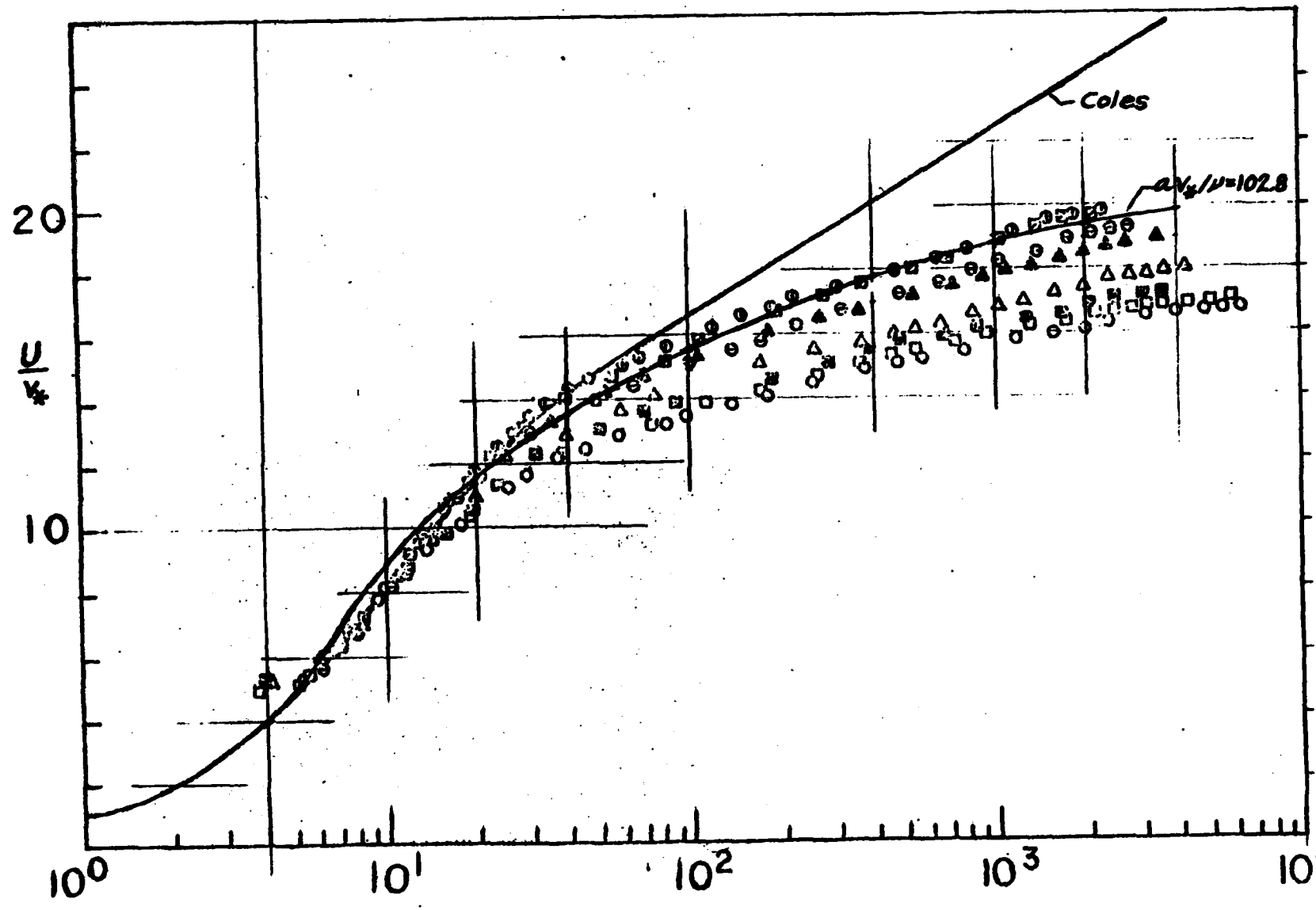

Figure A2-4